

**Nicolae-Adrian Palusan**

ISSN 0350-350X  
GOMABN 55, 4, 280-294  
Original scientific paper

## **THE CONNECTION BETWEEN THE ELECTROCHEMICAL PROPERTIES OF METALS AND LUBRICANT RHEOLOGY IN CYLINDRICAL TAYLOR-COUETTE FLOW**

### *Abstract*

*The behavior of fluids in developing flow regions is of importance for many applications of drag reducing surfactant solutions, such as hydronic cooling and heating systems. Moreover is the chemical or electrochemical effect important, which appears at the interface between the metal surface and fluid. A very thin layer of fluid is supposed to be adsorbed on the metal surface as a consequence of this chemical or electrochemical effect. A specific Couette rheometer has been developed for the purpose of emphasizing that chemical or electrochemical effect in the cylindrical Taylor-Couette flow. In order to perform time-dependant viscometer measurement on viscous fluids, the fluids having a non-Newtonian behavior related to a long "characteristic time", a new type of viscometer with a sensitive dynamic has been developed in a cooperation between our Research laboratory, the Tribology laboratory of Technical University of Brasov and the Chemical Instruments laboratory of Timisoara Technical University.*

*The Couette cell is made of two moving concentric cylinders (the outer cylinder is the driver and the inner cylinder is driven). The inner cylinder is moving supported by an air bearing (frictions are avoided) and is interchangeable so that there can be variations of the gap dimensions (between the cylinders) and the materials which are used to build the inner cylinder. When a viscous fluid is sheared between two concentric cylinders undergoing differential rotation, the free surface of the fluid is deformed as a consequence of that shearing motion, as well as of both gap dimension (between the cylinders) and the material which is used to build the inner cylinder (different surface tension effect for different material). This paper is a rheological study on fluids (in general) and lubricants (in particular) in Taylor-Couette flow.*

**Keywords:** Couette apparatus; Taylor-Couette flow; shear stress; air bearing; apparent viscosity; rotational viscosity; potential of zero charge

## 1. Introduction

The Couette-Taylor problem concerns the flow between independently rotating cylinders (fig. 1). The flow between rotating cylinders is remarkable in terms of the fact that slow increase of the speed of the moving cylinder gives rise to a progression of clearly distinguishable fluid states that have increasing complexity [1]. The fluid experiences all the shearing stresses between their maximum and minimum (or stationary) values in one passage, so it can bring to light any dependence of the apparent viscosity on the velocity gradient.

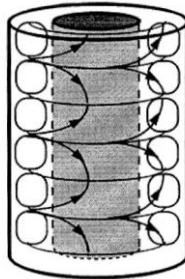


Figure 1: Schematic representation of Taylor Couette flow between two independently rotating cylinders

But before using non-Newtonian fluids, the behavior of the apparatus has been checked with Newtonian fluids, respectively the reproducibility and accuracy of the results and the validity of the hypothesis, which has been tested by deriving the equation of the rotor). Thereby it was experimentally proved that the motion of the new viscometer is in very close accordance with the theoretical calculations.

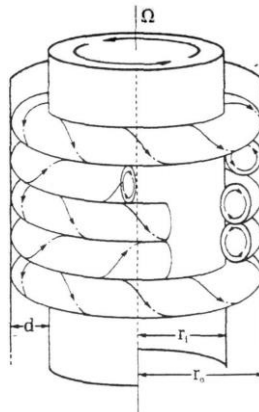


Figure 2: Schematic representation of Taylor vortices in Taylor-Couette flow between two cylinders; one of them is rotating.

The results concerning all the technical aspects will be published later, the present paper will concern only the theoretical derivations of the motion equations and the potential influence of the covering material nature (chemical composition) of the moveable cylinder on fluid flow (in order, on the Taylor vortices (fig. 2)). However, a schematic description of the viscometer is given below, in order to explain the origin of the boundary conditions. It is also necessary to define the electrochemical parameter which can explain the different rheological behaviors of the testing fluids in the Couette rheometer, because of the different inner cylinders (each from a different material).

**1.1 Principle of the apparatus**

The Couette apparatus is made of two independently rotating cylinders [the outer cylinder with radius  $r_2$  (at the fluid contact) is the driver and the inner cylinder with height  $h$  and radius  $r_1$  is driven by the fluids between cylinders] moved by an asynchronous electrical motor. The inner cylinder is sustained by an air bearing. Thus, the resistance against the moving of the inner cylinder can be considered negligible (fig. 3). Angular velocities of the outer and inner cylinders are  $\Omega_2$  and  $\Omega_1$ , and the total inertia moment is  $I_0$ .

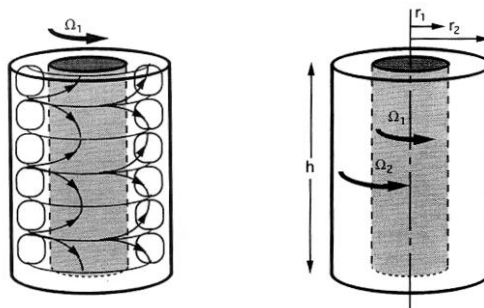


Figure 3: The defining parameters of Taylor-Couette flow between two independently rotating cylinders

**1.2 The boundary conditions**

If  $\eta$  is the shear viscosity of the fluid, the shearing stress on the driver cylinder is:

$$\tau = \eta r_1 \left( \frac{\partial \Omega}{\partial r} \right)_{r_1} \tag{1}$$

thus for a simple case of relaxation, neglecting the air bearing resistance, the motion is described by the following relation (from the start of rotation of the driver cylinder):

$$I_0 \left( \frac{\partial \Omega}{\partial t} \right)_{r_1} = 2\pi h r_1^2 \tau \tag{2}$$

or

$$\left(\frac{\partial\Omega}{\partial t}\right)_{r_1} = \frac{2\pi hr_1^3}{I_0} \eta \left(\frac{\partial\Omega}{\partial r}\right)_{r_1} \quad (3)$$

In accordance with the previous hypothesis, in general case, the first boundary condition can be written as:

$$\left(\frac{\partial\Omega}{\partial t}\right)_{r_1} = K_1 \left(\frac{\partial\Omega}{\partial r}\right)_{r_1} - K_2(\Omega)_{r_1} + K_3. \quad (4)$$

The other conditions are the common ones:

$$\Omega(r_2, t) \equiv \Omega_2, \quad (5)$$

$$\Omega(r, t = 0) = \Omega_1(r). \quad (6)$$

For a Newtonian fluid the classical differential equation:

$$\frac{1}{r^3} \frac{\partial}{\partial r} \left[ r^3 \frac{\partial\Omega}{\partial r} (r, t) \right] = \frac{1}{\nu} \frac{\partial\Omega}{\partial t} (r, t), \quad (7)$$

must be solved;  $\rho$  is the mass of unit volume of the fluid, and  $\nu = \eta/\rho$ .

The parameters  $K_1$ ,  $K_2$  and  $K_3$  depend on the morphological parameters of the moving system:

$$K_1 = \frac{2\pi hr_1^3}{I_0} \eta, \quad K_2 = \frac{\lambda}{I_0} + K_a, \quad K_3 = \frac{\lambda\Omega_2}{I_0}.$$

$\lambda$  is proportional to  $\Omega_2$  at the rotation starting stage, whereas it is a variable function  $-f(\Omega_2 - \Omega_1)$  during rotation;  $K_a$  represents the viscous resistance of air bearing.

## 2. The equations and the parameters of this flow

As shown in fig. 1, both radii of the inner cylinder  $r_1$  and outer cylinder  $r_2$  and the height of the flow region between the cylinders specify the geometry of the system. The inner cylinder rotates with angular velocity  $\Omega_1$ , which is determined by convention to be positive. The outer cylinder rotates with angular velocity  $\Omega_2$ , which is negative when its rotation direction is opposite to the rotation direction of the inner cylinder. If an incompressible fluid is considered, the density and temperature remain constant. The flow state is specified by a velocity field  $u = (u, v, w)$  and the pressure field  $p$ . In cylindrical coordinates,  $u$ ,  $v$ , and  $w$  are the radial, azimuthal and axial velocity components. These fields are governed by the Navier-Stokes and continuity equations:

$$\frac{\partial u}{\partial t} + (u \cdot \nabla)u = -\nabla p + \frac{1}{\text{Re}_1} \nabla^2 u, \quad (8a)$$

$$\nabla \cdot u = 0. \quad (8b)$$

These equations are expressed in non-dimensional form: distance is in units of the gap between cylinders,  $d = r_1 - r_2$ , and velocity is measured in units of  $\Omega_1 r_1$ . Consequently, time is measured in units of  $d/(\Omega_1 r_1)$ , which is called an inertial or advective time scale, and pressure is measured in units of  $\rho(\Omega_1 r_1)^2$ . It is sometimes convenient to measure time in units of a viscous diffusion time  $d^2/\nu$ , where  $\nu$  is the kinematical viscosity of fluid [2]. The Reynolds number is defined by  $Re_1 = \Omega_1 r_1 d/\nu$  and is usually the measurement of the relative strength of inertial to viscous forces. Here it may also be represented as the ratio of the viscous diffusion time ( $d^2/\nu$ ) to the inertial time scale  $d/(\Omega_1 r_1)$ . Besides the Reynolds number proportional to  $\Omega_1$ , other dimensionless parameters of the system are the radius  $\alpha = r_2/r_1$ , the aspect ratio  $\Gamma = h/d$ , and the speed ratio  $\beta = \Omega_2/\Omega_1$ . Sometimes, it is convenient to measure the outer cylinder angular velocity by a second Reynolds number  $Re_2 = \Omega_2 r_2 d/\nu$ . However, viscosity  $\nu$  is often the least accurately known quantity in describing experimental conditions. The use of the velocity ratio  $\beta$  rather than  $Re_2$  can minimize the propagations of this uncertainty.

Near transition there are physical reasons for replacing the original Reynolds number  $Re_1$  with another parameter – the Taylor number that is a more specific measure of relative time scale in rotating flows. The Taylor number is:

$$Ta \equiv \frac{4\Omega_1 d^4}{\nu^2} \frac{\Omega_1 r_1^2 - \Omega_2 r_2^2}{r_2^2 - r_1^2} = 4(Re_1)^2 \frac{1 - \alpha}{1 + \alpha} \left( 1 - \frac{\beta}{\alpha} \right) \tag{9a,9b}$$

Solutions to equations (9) must satisfy non-slip boundary conditions at the walls. In dimensionless form, this means that  $(u, v, w) = (0, 1, 0)$  at the inner cylinder radius  $r = \alpha/(1 - \alpha)$ , and  $(u, v, w) = (0, \beta/\alpha, 0)$  at the outer cylinder radius  $r = 1/(1 - \alpha)$ . To describe finite-length cylinders, additional boundary conditions will have to be imposed at  $z = \pm \Gamma/2$ . If the idealization of infinitely long cylinders is made, there is a closed-form solution for a state of flow between the cylinders for any set of rotation rates. The fluid moves azimuthally around the cylinders, in layers of motion that depend only on the radius. This is the "laminar Couette flow". If  $(U, V, W)$  represent radial, azimuthal and axial components of velocity and  $P$  represents the pressure, the basic flow is given by:

$$V = Ar + \frac{B}{r}, U = W = 0, \tag{10a}$$

$$P = P_0 + \int_{r_1}^{r_2} \frac{V^2(r)}{r} dr. \tag{10b}$$

The coefficients  $A$  and  $B$  are determined by the non-slip boundary conditions at the walls:

$$A = \frac{\beta - \alpha^2}{1 - \alpha^2} \cdot \frac{1 - \alpha}{\alpha}, \tag{11a}$$

$$B = \frac{1-\alpha}{1-\alpha^2} \cdot \frac{\alpha}{1-\alpha}. \quad (11b)$$

The basic flow is in fact produced in good approximation between finite, but sufficiently long cylinders providing the rotation rates are slow. An important feature of this flow is its complete lack of features. It has the same symmetry as the imposed conditions, meaning that it is invariant under translations in the axial rotation towards azimuthal direction and shifts in time. This illustrates a key aspect of non-equilibrium physics – if the stress is small enough, the system responds in a unique way that has the same symmetry as the imposed stress and remains in a state that is not far removed from thermodynamic equilibrium. This state of motion is sometimes referred to as the “thermodynamic” branch.

Laminar Couette flow finds many uses as a state of well-defined shear, for example in studying the effect of shear of biological specimens and in understanding the relation between stress and rate of strain for more complex fluids, such as polymers and suspensions. Although the state of motion is simple, when the cylinders are concentric, an intentional misalignment of axes and modulation of the cylinders rotation can generate flows of considerable spatial complexity.

### 3. The electrochemical parameter that influences this flow

Consider a cell which has a metal immersed in a solution of its ions and a standard hydrogen electrode. The cells electromotive force equals the electrode potential  $\varepsilon_{LM}$  of metal M, on the arbitrary hydrogen scale written as:

$$\varepsilon_{LM} = g_{LM} + g_{MPt} + g_{PtL}, \quad (12)$$

and consists of three electrochemical potential terms, including the Galvani potential across the boundary between the metal electrode and platinum electrode. The Galvani potential across the water based solution-metal interface may be represented as a sum of four terms:

$$g_{LM} = g_{LM(q)} + g_{LM(s)} + g_{LM(dip_1)} + g_{LM(dip_2)}, \quad (13)$$

where subscripts  $q$ ,  $s$ ,  $dip_1$  and  $dip_2$  represent the potential-determining ions, specifically adsorbed ions, the dipoles of the solvent and the dipoles of any unionized organic substance. The terms  $g_{LM(dip_1)}$  and  $g_{LM(dip_2)}$  include the dipole-layer component which is present in the metal and which is due to the divergence of the electric centers of gravity of the ions and electrons in the surface layer. If  $g_{LM(q)} = 0$ , the metal surface has no charge and the electrode potential will correspond to the zero-charge potential:

$$\varepsilon_{LM} = g_{LM(s)} + g_{LM(dip_1)} + g_{LM(dip_2)} + g_{MPt} + g_{PtL} \equiv_{LM} \varepsilon_{q=0} \quad (14)$$

In accordance with what has been said above, the uncharged surface potential of metals depends on the nature of the metal, the reference electrode used the solvent nature and the solution composition. For the selected metal and solvent the value of potential  ${}_{LM}\mathcal{E}_{q=0}$  may be different, depending on  $g_{LM(s)}$  (i.e. the nature and concentration of capillary-active ions) and  $g_{LM(dip_2)}$  (i.e. the nature and concentration of capillary-active dipolar molecules). If, however, not only  $g_{LM(q)}$  is equal to zero, but  $g_{LM(s)}$  and  $g_{LM(q)}$  as well, i.e. if there are no capillary-active particles in the solution except the molecules of solvent L, then the following equation should be written in place of equation (14):

$$\mathcal{E}_{LM} = {}_{LM}\mathcal{E}_{q=0} = {}_N g_{LM(dip_1)} + g_{MPt} + g_{PtL} \equiv {}_{LM}\mathcal{E}_N \quad (15)$$

It can be seen from equation (15) that this partial value of the uncharged surface potential (i.e. the null point  ${}_{LM}\mathcal{E}_N$ ) must be a constant because it equals the sum of three constant quantities.

The null point may also be expressed in terms of the corresponding Volta potentials:

$${}_{LM}\mathcal{E}_N = {}_N\psi_{LM} + \psi_{PtM} + \psi_{PtL}. \quad (16)$$

Here the metal-solution Volta potential must be a strictly definite quantity ( ${}_N\psi_{LM}$ ) corresponding to the difference of external potentials between metal M and the solution, in which the potential of the metal is at null point. The thus determined null point has been chosen as the zero for the correlative (also known as reduced) scale of potentials proposed by Antropov [5].

The  $\varphi$  potential in the correlative scale is defined as the difference between the potential of an electrode under given conditions and its null point:

$$\varphi = \mathcal{E} - \mathcal{E}_N. \quad (17)$$

The two terms on the right side of the equation (17) must naturally be expressed on the same scale (e.g. on hydrogen scale); the value of the  $\varphi$  potential is independent of the chosen arbitrary or relative scale. Since the values of  $\mathcal{E}_N$  (experimental zero-charge potential of metals in aqueous solutions), are different for different metals [5] according to Trassati, each metal will have its own correlative scale based on its null point or potential of zero charge (the potential of the electro - capillary maximum of any metal). The correlative or  $\varphi$  scale of potentials is thus different from any arbitrary and the absolute scale of potentials.

This distinction is clearly seen in comparing the values of standard electrode potentials of some metals on hydrogen, absolute and reduced scales (Table 1).

Table1: Standard electrode potential and null point

Electrode	Hydrogen scale, $\varepsilon$ (V)	Absolute scale*, $\varepsilon_N \varepsilon_0$ (V)	Experimental Zero-charge Potentials scale, $\varepsilon_N$ (V)	Correlative scale, $\varphi$ (V)
Zn <sup>2+</sup> /Zn	-0.76	-0.76-(-0.20)=-0.56	-0.63	-0.76-(-0.63)=-0.13
Cd <sup>2+</sup> /Cd	-0.40	-0.40-(-0.20)=-0.20	-0.70	-0.40-(-0.70)=+0.30
Tl <sup>2+</sup> /Tl	-0.34	-0.34-(-0.20)=-0.14	-0.80	-0.34-(-0.80)=+0.46
Hg <sub>2</sub> <sup>2+</sup> /Hg	+0.80	+0.80-(-0.20)=+1.00	-0.20	+0.80-(-0.20)=+1.00
Fe <sup>2+</sup> /Fe	-0.44	-0.44-(-0.20)=-0.24	±0.00	-0.44-(-0.00)=-0.44
Ag <sup>+</sup> /Ag	+0.80	+0.80-(-0.20)=+1.00	-0.40	+0.80-(-0.40)=+1.20
Au <sup>3+</sup> /Au	+1.50	+1.50-(-0.20)=+1.70	-0.05	+1.50-(-0.05)=+1.45
Cu <sup>2+</sup> /Cu	+0.34	+0.34-(-0.20)=+0.54	+0.26	+0.34-(-0.26)=+0.60
Ni <sup>2+</sup> /Ni	-0.25	-0.25-(-0.20)=+0.05	-0.06	-0.25-(-0.06)=-0.19
Cr <sup>3+</sup> /Cr	-0.71	-0.71-(-0.20)=-0.51	-0.45	-0.71-(-0.45)=-0.26

\* This scale is also called Oswald scale of potentials. Since the potential of the electro-capillary maximum for mercury in solutions of capillary-inactive substances is about -0.20 V on the hydrogen scale, it follows, according Oswald.

It can be seen from Table 1 that in the hydrogen and absolute scale the arrangement of the metals in order of increasing positive value of standard electrode potential and differences between the values of two electrode potentials remain the same. In the correlative scale of potentials the order of arrangement of metals and the differences in values of their standard electrode potentials are quite different since the physical meaning of the potential in any arbitrary (and in absolute) scale and in the correlative scale is radically different. The potentials expressed on the arbitrary scale are reckoned from its own zero, which is the null point of the electrode metal. It will therefore be wrong to use the  $\varphi$  scale of potentials for solving problems associated with the thermodynamics of electrochemical systems or with electrode equilibrium and to use it instead of the hydrogen scale or the  $\varepsilon$  scale of potentials. The correlative scale does not enable us to determine, for example, the direction of a reaction and the electromotive force of an electrochemical system in equilibrium with two electrodes of known  $\varphi$  potential. This task is easily handled with the aid of the  $\varepsilon$  scale. The potential on the  $\varepsilon$  scale however yields no information about the charge of metal surface, the double-layer structure, or the most probable electrical nature of the particles which are preferentially adsorbed on the electrode surface under given conditions. These data are especially important and can be obtained by using the  $\varphi$  scale of potentials.

Proceeding from the definition of the  $\varphi$  potential (17) and taking into account that the  $\varepsilon$  potential, which is different from the  $\varepsilon_N$  potential, is given by the equation:

$$\varepsilon_{LM} = g_{LM(q)} + g_{ML(dip_L)} + g_{MP_L} + g_{PL}, \quad (18)$$

one can obtain the following expression for the electrode potential on the  $\varphi$  scale<sup>1)</sup>:

$$\varphi = \varepsilon - \varepsilon_N = g_{LM(q)} + g_{LM(dip_L)} - {}_N g_{LM(dip_L)}, \quad (19)$$

<sup>1)</sup> Equations (18) and (19) refer to solutions containing no capillary-active substances ( $g_{LM(s)} = 0$ )

Equation (19) allows one to view the electrode potential on the  $\varphi$  scale as a measure of the charge on the metal (the intensity of the double-layer  $g_{LM(q)}$ ) and also as a measure of the variation in orientation of polar solvent molecules at the metal-electrolyte interface upon transition from the null point to the given value of potential (the difference between the quantities  $g_{LM(dip_L)}$  and  ${}_N g_{LM(dip_L)}$ ). There are grounds to believe that the orientation of solvent dipoles on a charge-free metal surface depends little on its nature and that the value of  ${}_N g_{LM(dip_L)}$  is approximately the same for all metals in aqueous solutions. For example, if for metal 1 and metal 2:

$$\varphi_1 = \varphi_2 \quad (20)$$

or:

$$g_{LM_1(q)} + g_{LM_1(dip_L)} - {}_N g_{LM_1(dip_L)} = g_{LM_2(q)} + g_{LM_2(dip_L)} - {}_N g_{LM_1(dip_L)} \quad (21)$$

then:

$$g_{LM_1(dip_L)} - {}_N g_{LM_1(dip_L)} = g_{LM_2(dip_L)} - {}_N g_{LM_2(dip_L)}, \quad (22)$$

since the charge of dipole orientation depends only on the electrode charge, and:

$$g_{LM_1(q)} = g_{LM_2(q)}. \quad (23)$$

The equality of the  $\varphi$  potentials of two or more metals is an indication that the ionic potential differences and the charges on the surfaces of these metals are approximately equal. The same inference can be made if the potential is expressed in the terms of the corresponding Volta potentials. Because the values of the  $\varphi$  potential are known, one can therefore compare different metals from the viewpoint of their charges and the conditions of adsorption of capillary-active substances on them.

## 4. Experimental procedure

### 4.1 Experimental apparatus

The Couette apparatus is made of a Couette cell, the drive-rotating device of the outer cylinder and a group of interchangeable inner cylinders with various radii, cover material and roughness of the cylindrical surface. This paper focused only on four inner cylinders with various cover material of the cylindrical surface (gold, silver, copper, chromium nickel and steel).

All cylinders had the same cylindrical surface roughness (very low  $R_a = 0.24 \mu\text{m}$ ) for the study of the influence of these materials on the flow. The construction of Couette cell and Couette apparatus are illustrated in Figure 4.

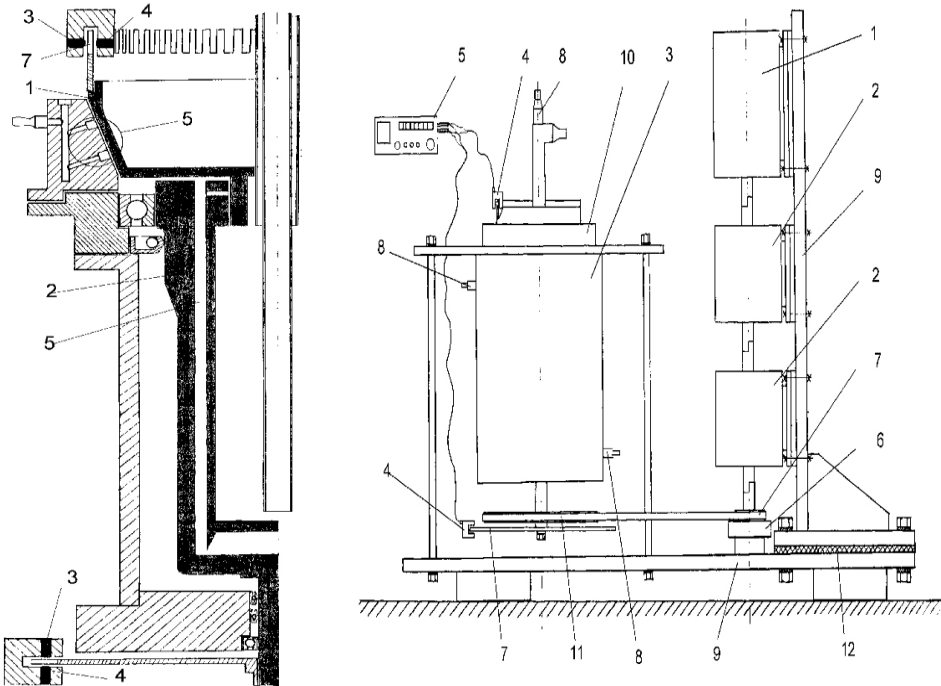


Figure 4: Schematic representation of Couette cell and Couette Apparatus

The inner cylinder is supported and sustained by an air bearing. The outer cylinder is made of steel having an inside diameter of 70 mm. All four inner cylinders were made of steel and three of them were covered by PVD (physical vapor deposition) with an extremely thin monolayer of gold, copper and nickel. The outside diameter of each inner cylinder is 68 mm, having radius ratio  $\alpha = 1.029$  and aspect ratio  $\Gamma = 2.558$ . For producing the stability flow conditions, it is necessary to respect the requirements from Figure 5.

The outer cylinder is securely locked in place on the drive shaft, which had a mounted belt wheel outside the Couette cell. The wheel transmitted the motion by an asynchronous electrical motor. The temperature of the Couette cell can be adjusted. An ultra-thermostatic system is connected to the Couette cell. The temperatures of both cylinders can be adjusted and set up.

The rotational speeds were separately measured by an optic-electronic system [3]. This system was connected to a personal computer for data processing.

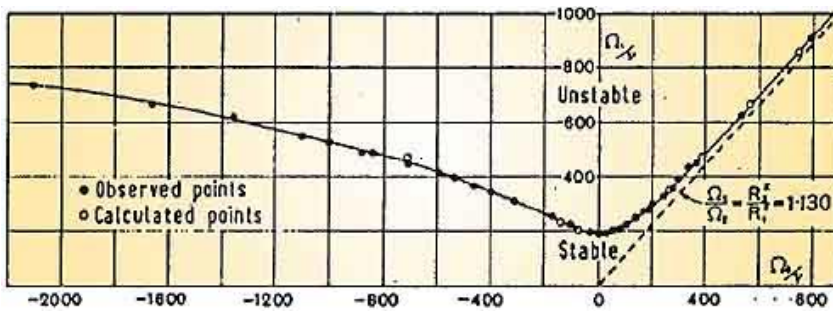


Figure 5: Stability domains in Taylor-Couette Flow

#### 4.2 Taylor–Couette stability diagram

This plot, from Taylor’s 1923 paper on the instability of flow between two coaxial rotating cylinders, was the first example of a theoretical calculation of a fluid-flow instability that quantitatively agreed with experiments. The stability boundary as a function of the rotation speed of the outer cylinder (ordinate) and inner cylinder (abscissa) is shown. The dashed line  $\Omega_1 r_1^2 = \Omega_2 r_2^2$  is a previous theory by Lord Rayleigh. The solid points represent experimental measurements; the open points theoretical calculations of the stability boundary. Due to the complexity of numerically evaluating the formulas from the theoretical calculations, there are more experimental data points than theoretical points, as well represented in Figure 5.

#### 4.3 Experimental results

Experiments were carried out with two different fluids, a 90 % water and 10 % glycerin solution and an emulsion with 5 % mineral oil (contained by a non-ionic emulsifier). All six cylinders were used with all two fluids at four different rotational speeds of the outer (driver) cylinder only in counter - clockwise direction. Because the gap between the cylinders was thin (only 1 mm), the Weissenberg effect (climbing of the fluid up the inner cylinder) was neglected. The measurements were carried out at 25 °C. Under these circumstances, for a small amount of shear stress, the rheological behavior of the two fluids could be considered of Newtonian type and the fluid flow between the cylinders had to be considered laminar (stable Couette laminar flow) for a 1 mm gap. The dynamical viscosity of the two fluids was measured separately with a laboratory viscometer and with the experimental Couette apparatus at 25 °C. The values of the measurements were very close for each fluid. The equation for the calculation of the apparent dynamic viscosity by the experimental Couette apparatus is:

$$\eta_a = \frac{m_{\beta} \Omega_1^2}{4\pi(\Omega_2 - \Omega_1)h} \cdot \frac{r_2 - r_1}{r_2 + r_1}, \tag{24}$$

It represented the equation of calculating viscosity resulted from the mathematical model of this apparatus. The measured viscosities were 12.48 cP, for the 90 % water and 10 % glycerin solution, and 3.56 cP for 5 % mineral oil and water emulsion when the laboratory rheometer was used, whereas when the Couette apparatus with the steel inner cylinder was used 1.53 cP and 3.58 cP, respectively. To establish the influence of the covering material type, the Taylor number ( $Ta$ ) was calculated for each test by equation (9). The evolution by time of the cylinder rotating speed was plotted as diagrams in Figures 6.1 - 6.5.

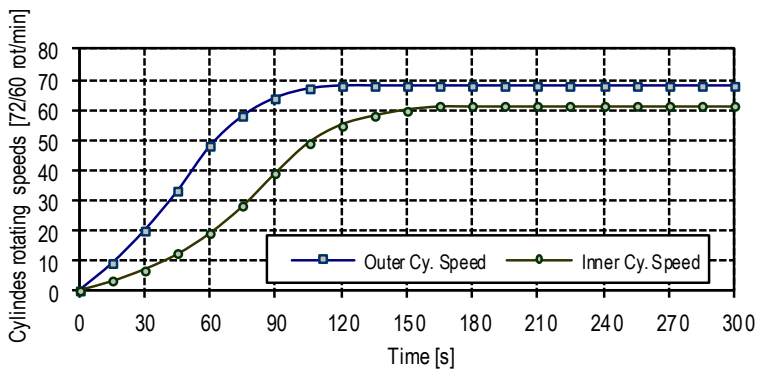


Figure 6.1: Cylinders rotating speed vs time (water-glycerin solution) - steel inner cylinder

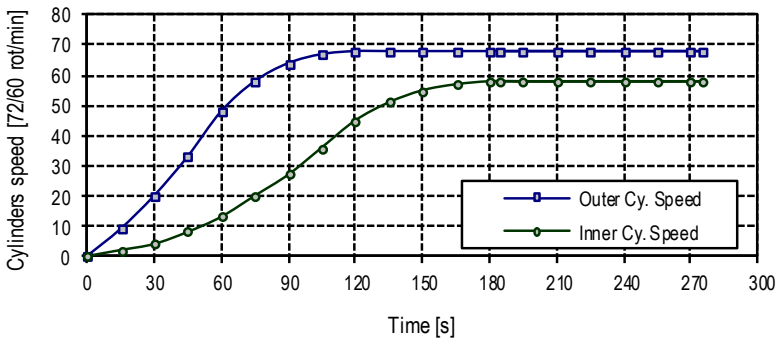


Figure 6.2: Cylinders rotating speed vs time (water-glycerin solution) - copper inner cylinder

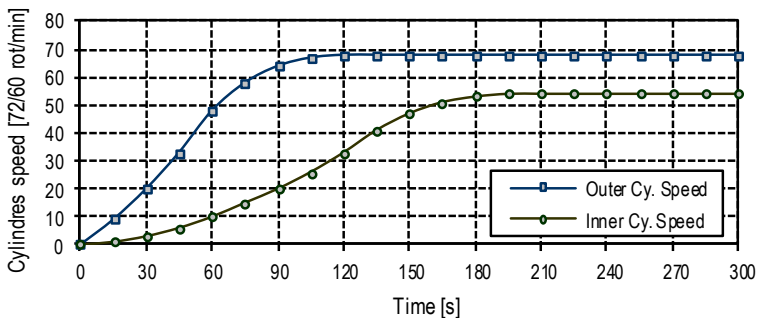


Figure 6.3: Cylinders rotating speed vs time (water-glycerin solution) - nickel inner cylinder

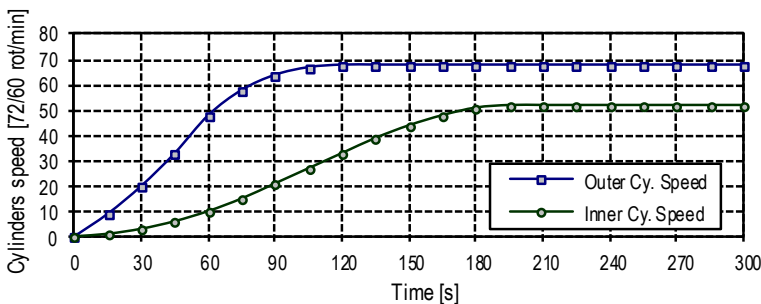


Figure 6.4: Cylinders rotating speed vs time (water-glycerin solution) - chromium inner cylinder

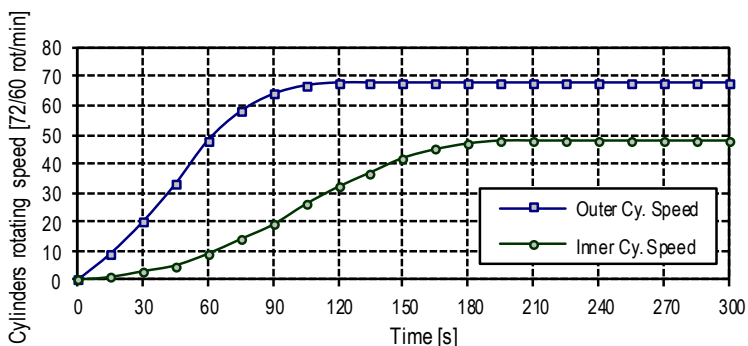


Figure 6.5: Cylinders rotating speed vs time (water-glycerin solution) - silver inner cylinder

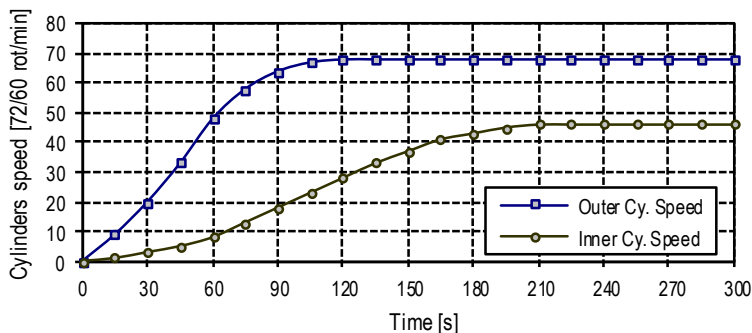


Figure 6.6: Cylinders rotating speed vs time (water-glycerin solution) - gold inner cylinder

There are noticeable differences among the evolutions of four inner cylinder rotation speeds for both fluids. The increase of the inner cylinder rotation speed was very different for each type of material in the transition interval. Also the difference  $\Omega_2 - \Omega_1$  in the stationary interval increased in the following order: gold – silver – chromium – nickel – copper – steel. The same situation was observed for all five rotation speeds of the outer cylinder (50, 100, 150 and 200  $\text{min}^{-1}$ ) and for both fluids (as they are both water based). Under these circumstances, the principal physical-chemical behavior was imposed by water. Theoretically, the Taylor number had to be the same for all material types of cylinders (for each test); however, the calculated Taylor numbers were different. Different speed ratios were obtained,  $\beta_{\text{Au}} = 1.255$ ,  $\beta_{\text{Ni}} = 1.200$ ,  $\beta_{\text{Cu}} = 1.173$ ,  $\beta_{\text{Fe}} = 1.125$ . The molecules of both water and glycerin have polar electric character, but water molecule polarity is stronger. Water as well as glycerin form molecular aggregates (from 12 to 100 molecules) with good physical adsorption potential and chemical affinity for metals with electrochemical potential. The adsorption is superficially carried out as a chemical reaction. If temperature increases, the number of molecules in the aggregates decreases so that it is possible that the Taylor number for all four material types of the inner cylinder is the same at temperatures over 60 °C. The number of Taylor vortices (in laminar period) increased proportionally to the speed of the inner cylinder. It is possible that a significant physical-chemical phenomenon is formed at the boundary.

Gold is completely chemically inactive to water and is not wetted by it. Silver has a very low chemical activity and its zero-charge potential is also very low. Chromium and nickel are chemically passive to water (because they form complex combinations with inactive chemical substances), but are wetted by it. The difference between them is the smaller value of the zero-charge potential for chromium. Copper and steel are chemically active to water and are wetted by it. Steel (iron) is more electropositive than copper.

These characteristics could be explained by the rheological behavior in the first stage of this research program. The zero-charge potential has important influences on the molecular adsorption tendency. The values from Table 1 reflect a proportional connection between the potential  $\varphi$  and the differences  $\Omega_2 - \Omega_1$ . Additionally, in the emulsion case, the effect of the emulsifier, the dispersion level and level of shear stress of the emulsion particles were significant. The particles also introduced a geometric effect, but the rheological behavior in time was in the same direction.

In all these cases, the Langmuir theory could be applied because it refers to the adsorption of one molecular (aggregate) layer to a metallic surface [4]. In this situation the boundary conditions could be changed and the flow, especially between very close metallic surfaces, could be considered a particular case.

## 5. Conclusion

This paper is part of a research project concerning the physical-chemical effect in Taylor–Couette flow. The water-glycerin behavior can be explained by the adsorption of molecular aggregates of water, glycerin or/and mixed combination. In the emulsion case, because of the difference in conformational entropy between regions of different shear, diffusion of viscous-elastic particles will occur towards low shear regions. This will decrease the viscosity in high shear regions and further increase local shear speed. As a result of that a part of emulsifier migrates to the inner cylinder wall eventually.

The results can be applied to study rheological and tribological behaviors of water based lubricants for metal working fluids and hydraulics of water based fluids.

## References

- [1] Ravey, J.C.; Dognon, M.: Transient Rheology in Couette Apparatus. *Rheologica Acta*, 19 (1980) 1, 51 – 59.
- [2] Tagg, R.: *The Couette-Taylor Problem*, Springer-Verlag, 4 (1994) 3.
- [3] Mason, T.G.; Weitz, D.A.: Optical Measurements of Frequency-Dependent Linear Viscoelastic Moduli of Complex Fluids. *Physical Review Letters*, 75 (1995) 14, 1250 – 1253.
- [4] Wang, J.; Xing, D.Y.: Coupling between a First-Order Gas-Liquid Phase Transition and a Second-Order Orientational Transition in Langmuir Monolayers. *Physical Review E*, 60 (1999) 6, 6951 – 6955.
- [5] Antopov, L.: *Theoretical Electrochemistry*, Mir Publisher (1977).

## Author

Dr. Nicolae-Adrian Palusan; E-mail: [adrian.palusan@total.com](mailto:adrian.palusan@total.com)  
Total Romania, 2, Stejarilor Street, 507055 Cristian - Brasov, Romania

**Received:** 20.10.2015.

**Accepted:** 30.4.2016.